# Fabrication and Performance of Diffractive Optics for Quantum Well Infrared Photodetectors

**F.S. Pool, D.W. Wilson, P.D. Maker, R.E. Muller, J.J. Gill, D.K. Sengupta, J.K. Liu, S.V. Bandara and S.D. Gunapala**

Center for Space Microelectronics Technology
Jet Propulsion Laboratory, California Institute of Technology
4800 Oak Grove Drive
Pasadena, California 91109

## ABSTRACT

Diffractive optical elements (microlenses) for quantum well infrared photodetectors (QWIPs) were fabricated by two techniques: 1) standard lithography of a binary optical structure and 2) PMMA pattern transfer for an analog diffractive optic structure. The binary lenses were fabricated by sequential contact lithography and etching using two binary masks. The analog diffractive lenses were fabricated in PMMA by direct-write e-beam lithography followed by acetone development. The resulting PMMA surface relief profile was transferred into the GaAs by dry etching. Both types of lenses were etching into GaAs using an electron cyclotron resonance (ECR) microwave plasma etching system. Although the lenses were fabricated accurately, the performance of the QWIPs was not improved as much as expected due to the angle-of-incidence sensitivity of the QWIP light-coupling grating. The lenses would have likely improved the performance of detectors capable of absorbing normally incident light.

*Keywords*: diffractive optics, multi-quantum-well, GaAs, PMMA

## 1. INTRODUCTION

In recent years, the rapid development of QWIP has demonstrated its applicability in long-wavelength(LW) and very-long-wavelength(VLW) infrared(IR) imaging and sensing arena. In a continuing effort to enhance the performance of QWIP detectors for NASA's IMAS project in the VLWIR region, we have been exploring many ideas which will increase specific detectivity (D*), namely the signal to noise ratio, of the detector. In particular the IMAS project requires a 15μm detector operating at 55 °K. The QWIP dark current is very high at this operating temperature. Therefore, we have been studying the possibility of using microlenses to reduce the detector area.

The general concept is to increase the signal output or decrease the dark current or both per detecting pixel. The work presented here is to increase the signal output by using a microlens to concentrate the photon flux. This will lead to a much smaller detector area requirement. Since the dark current is linearly related to the detector area, the dark current is decreased. Thus, achieving the goal of increasing the D*. The reduction of dark current can be expressed as the ratio of the area gain, $G_A$.[1] If d is the diameter of the focal spot and D is the pixel diameter, then $G_A = (D/d)^2 = [Dn_r f(\#)/F]^2$, where $n_r$ is the index of refraction, f(#) is the f number of the optical system and F is the focal length of the microlens. For example, if we let D = 2.44 λf(#) which the diameter of an Airy disk, then at 15 μm, D 73 μm. If we select F=125 μm then d 20 μ m. The dark current will improve by a factor of 13. If F=75 μm then d 12um, the dark current will improve by a factor of 37.

## 2. EXPERIMENTAL

### QWIP Fabrication

The QWIP structure is made up of multiple quantum wells of GaAs/AlGaAs sandwiched by two highly doped contact layers. The layers are grown using Molecular Beam Epitaxy. The detector is fabricated using simple contact photolithography. Three masking steps are involved. First, the grating for the detector is etched into GaAs using a Reactive Ion Etching system. Then the detector mesa is defined and etched in a wet chemical etchant. Finally, the Au/Ge ohmic contacts are evaporated onto the top and bottom contact layers.

### Microlens Fabrication

i) Binary Microlens

Four-level binary optic microlenses were fabricated by standard contact lithography,[2,3] using a two-mask photoresist pattern for plasma etching. The two-etch step process for fabrication of the four-level diffractive optics lenses created phase steps $d = \lambda/[2^2(n-1)]$, where n is the index of refraction of GaAs and $\lambda$ is the wavelength of the incident light for which the lens is optimized. Since these lenses were designed for incident light of 15μm the smallest feature size (outer zones) was approximately 4μm, making lithography relatively straightforward. Fabrication errors which resulted were level misalignment, etch depth errors, and limited resolution of outer zone features. The lenses were first fabricated and the QWIPs subsequently fabricated and aligned to the lenses through use of an infrared backside aligner to within 1 μm accuracy. The theoretical efficiency of a four-level diffractive optic lens in the scalar approximation is 81%. In this study microlenses were fabricated from 150x150μm to 350x350μm for infrared radiation to be focused on 75x75μm QWIP detectors, optimized for a peak wavelength of 14μm.

ii) Continuous Relief Fresnel Lens

In addition to the four-level lenses, continuous-relief lenses were fabricated by direct-write electron beam lithography[4-10] followed by transfer etching. The GaAs substrate was prepared for writing by spin coating 3 layers of PMMA to achieve a total thickness of approximately 2 μm. Each spin sequence included a bake-out for 60 minutes at 170° C. The pixel pattern was then written using the JEOL JBX-5DII electron beam tool operating at 50 keV in its low-resolution 4th lens mode. The field size – the distance spanned by deflection of the beam without need for stage motion – was 500 μm, and at 15 nA current, the beam spot was approximately 0.5 μm. Individual 1.0 μm square pixels were exposed by rastering this beam in steps of 0.2 μm, back and forth, with the dwell time adjusted to give the desired dose. This rastering, timing, and positioning were handled automatically by the JBX-5DII once given the coordinates and desired exposure for the pixel. After exposure, the PMMA film was developed in acetone for approximately 10 seconds. This was accomplished using a Solitec spinner equipped with an electronically controlled Tridak resist dispenser. The substrate was spun at 1000 RPM while the acetone was squirted down at the center of rotation. At the end of the 8 seconds, the acetone was abruptly cut off and replaced by a blast of dry nitrogen, which quenched the development and at the same time dried the surface of the PMMA. This process is monitored with a special development pattern. This pattern is measured with a special surface profiling tool at end of each development cycle. Subsequent developments in time steps controllable to 0.1 seconds were used to shim the surface profile to the desired depth. The process for fabrication of the continuous relief lens is given by the schematic representation in Figure 1. Figure 2 shows the surface of a 250 μm lens.

The plasma reactor used for transfer etching of both the binary and continuous lenses was a Plasma-Therm SLR 770 ECR microwave plasma etching system operating at 2.45GHz. The system is equipped with a backside He cooled stage for temperatures as low as 0C, rf bias (13.56MHz) for control of incident ion energies and loadlock for maintenance of UHV conditions in the process chamber. The base pressure of the etching chamber was approximately $9x10^{-8}$ Torr. Anisotropic etching of the structures defined in PMMA was performed using boron trichloride ($BCl_3$) and argon at a ratio of 1:4 and pressure of 1.0 mTorr, where the BCl3 is introduced through a gas ring approximately 2 cm above the substrate. The substrate temperature was maintained at 10C with a DC bias of -55V at 20W rf power. Given these conditions a GaAs:PMMA etch ratio of approximately 4:1 was achieved.

## 3. RESULTS

The responsivity was measured using a 1000K blackbody source and a grating monochromator. The responsivity of a 75μm x 75μm QWIP detector with and without a four-level 250 μm x 250 μm microlens is given in Figure 3. Although the effect of the microlens is evident through an increase in responsivity of approximately 2.7, the efficiency is far lower than a simple analysis would predict. The lenses were measured by Wyko Optical Profiler and a Tencor α-step profilometer and found to have etch depth errors of approximately 5% and misalignment error of approximately 1μm. The experiment was repeated with the continuous relief microlenses and the results were similar, even though the efficiency of the continuous lenses was likely higher than the 4-level lenses.

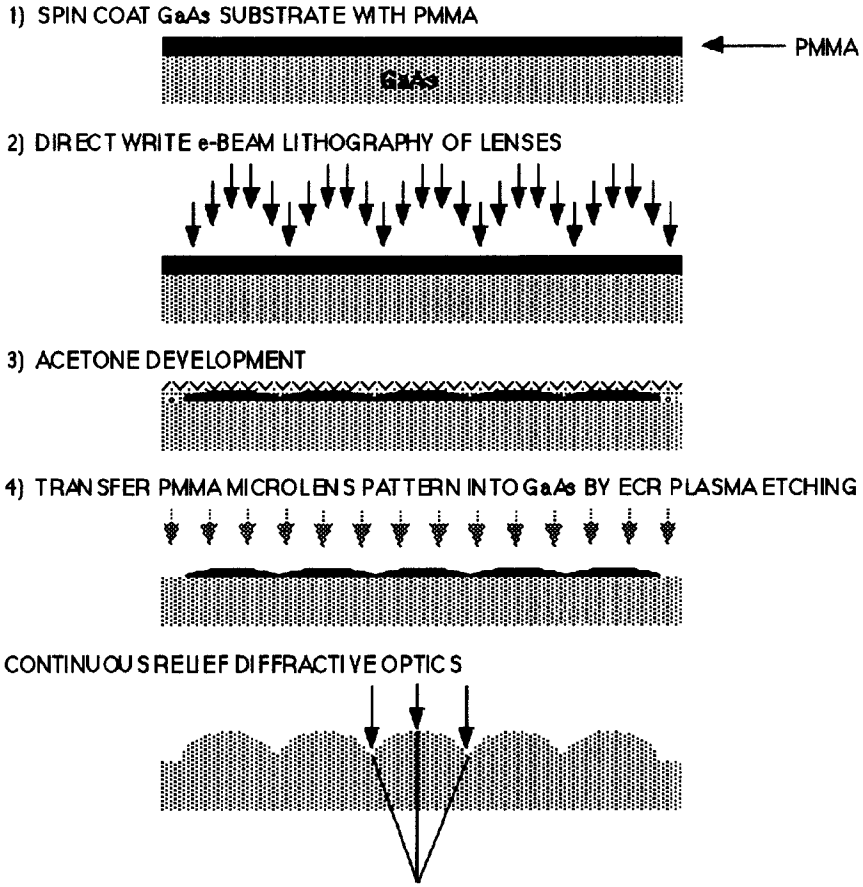


*Fig. 1. Schematic representation of the fabrication process for continuous relief lenses.*

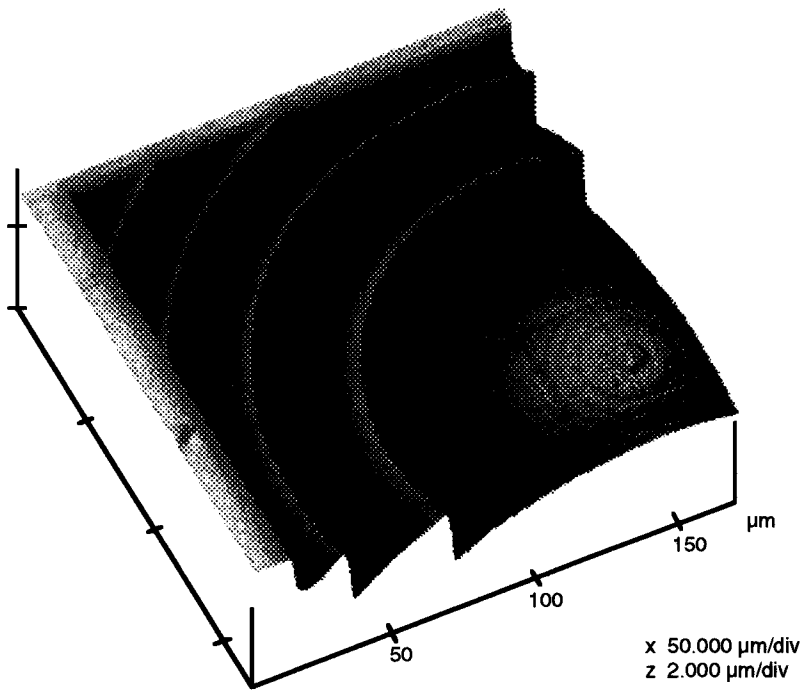


*Fig. 2. AFM image of a 250 µm microlens in PMMA.*

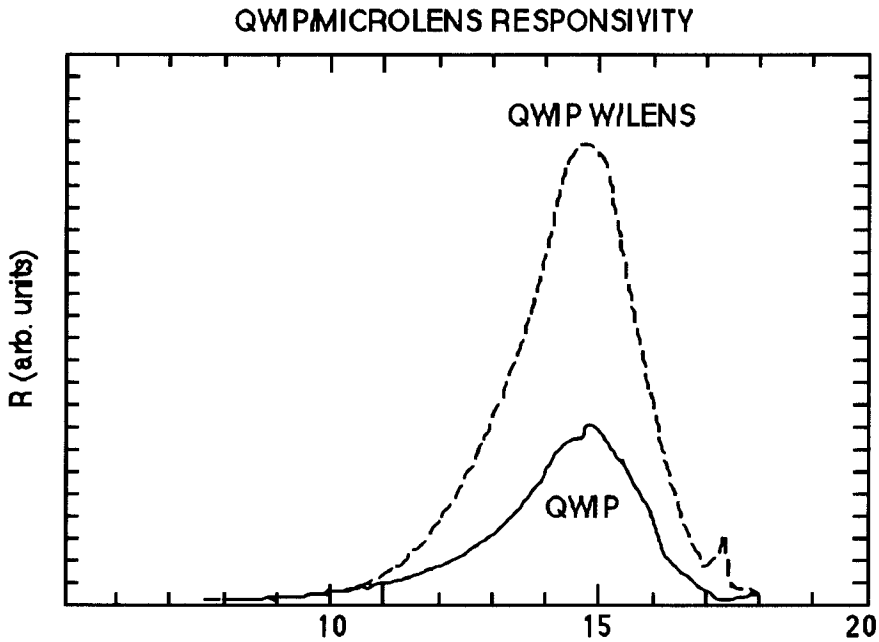


*Fig. 3. Relative responsivity of a QWIP with a lens and without a microlens*

## 4. DISCUSSION

The poor performance of the microlens-QWIP combination can be understood by analyzing the diffraction characteristics of the grating. The lens produces a cone of converging waves that are incident on the grating. Because the grating was optimized for normal incidence, the coupling of the angled waves into the desired polarization for QWIP absorption is severely degraded. There are two factors that influence the optical coupling: (1) the angles of the diffracted waves (grating orders), and (2) the efficiencies of the diffracted orders. The angles of the diffracted orders $\theta_m$ can be found directly from the grating equation,

$$\sin(\theta_m) = m\frac{\lambda_{GaAs}}{\Lambda} - \sin(\theta_{inc}), \quad m = 0, \pm 1, \pm 2, \cdot$$

where $\theta_{inc}$ is angle of incidence, $\lambda_{GaAs}$ is the wavelength inside the GaAs ($\lambda/3.1$), and $\Lambda$ = 4.85 μm is the grating period. Figure 4 illustrates angled incidence on a grating.

The efficiencies of the diffracted orders must be found using a rigorous electromagnetic analysis technique. In this study, rigorous coupled-wave analysis (RCWA)[11,12] was used to determine the efficiency of the grating as function of incident angle and wavelength. After the angles and efficiencies of the diffracted orders were found, the fields inside the quantum well stack were calculated. Because the QWIP can only absorb the component of the field perpendicular to the QW layers $E_\perp$, the integral of $|E_\perp|^2$ inside the QW region was taken as a measure of QWIP coupling efficiency. Figures 5 and 6 show the optical coupling and the order efficiencies as functions of incident angle. At 15 μm, the coupling is strongly peaked around normal incidence even though the diffraction efficiencies are not well optimized. At a shorter wavelength of 14.5 μm, the period to wavelength ratio is larger, allowing both the +1 and –1 orders to continue to propagate up to a few degrees off-normal as shown in Figure 6. This broadens the angular response, but because the angles of the diffracted orders are smaller, they do not couple as effectively into the QWIP and the peak response is reduced.

The focused field from the lens is actually not a plane wave, but it can be Fourier decomposed into an angular spectrum of plane waves. For a given lens, there is certainly an optimum grating period that maximizes the integrated product of the focused-field angular spectrum and the grating angular response. However, it is unlikely that a lens-grating combination will achieve the same responsivity as a grating optimized for normally incident plane-wave illumination. Furthermore, for the

lens-grating combination to effectively produce a higher signal-to-noise ratio, the area of the QWIP mesa must be reduced. In this situation, there may be too few grating periods for efficient diffraction.[13]

Although the microlens concept is not well suited for a QWIP detector, the concept described here can be soundly applied to normal incident absorbing infrared detectors.

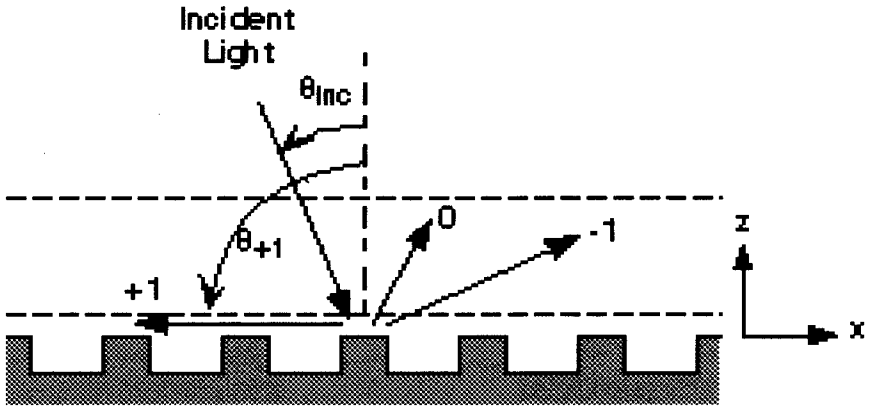


*Fig. 4. Diagram of angular incidence on the grating, where m=-1, 0, +1.*

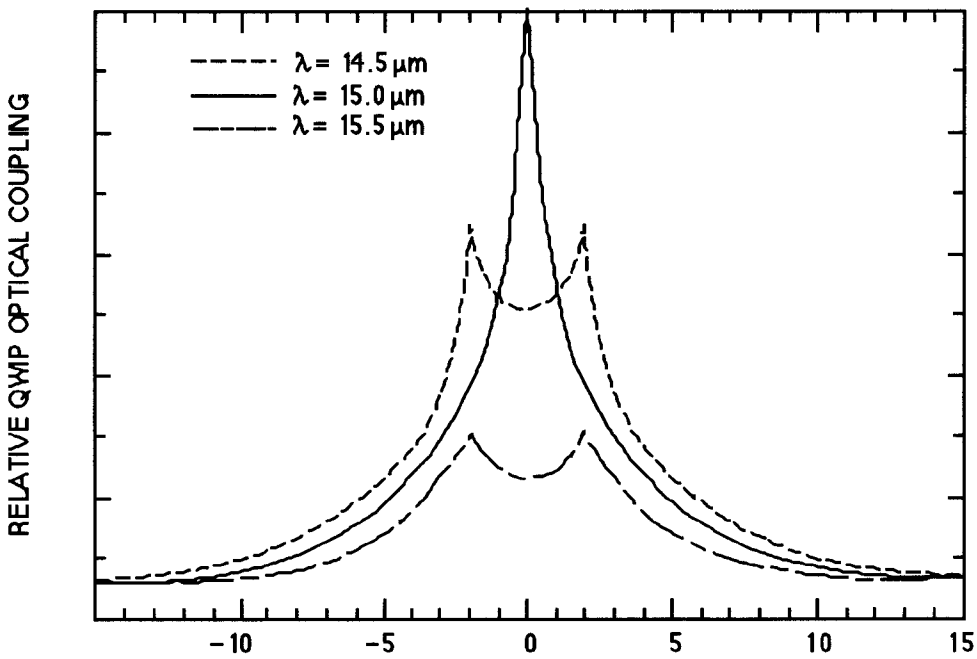


*Fig. 5. Relative optical coupling (see text for definition) as a function of incident angle at three wavelengths. All data was normalized by the 15 μm value at normal incidence.*

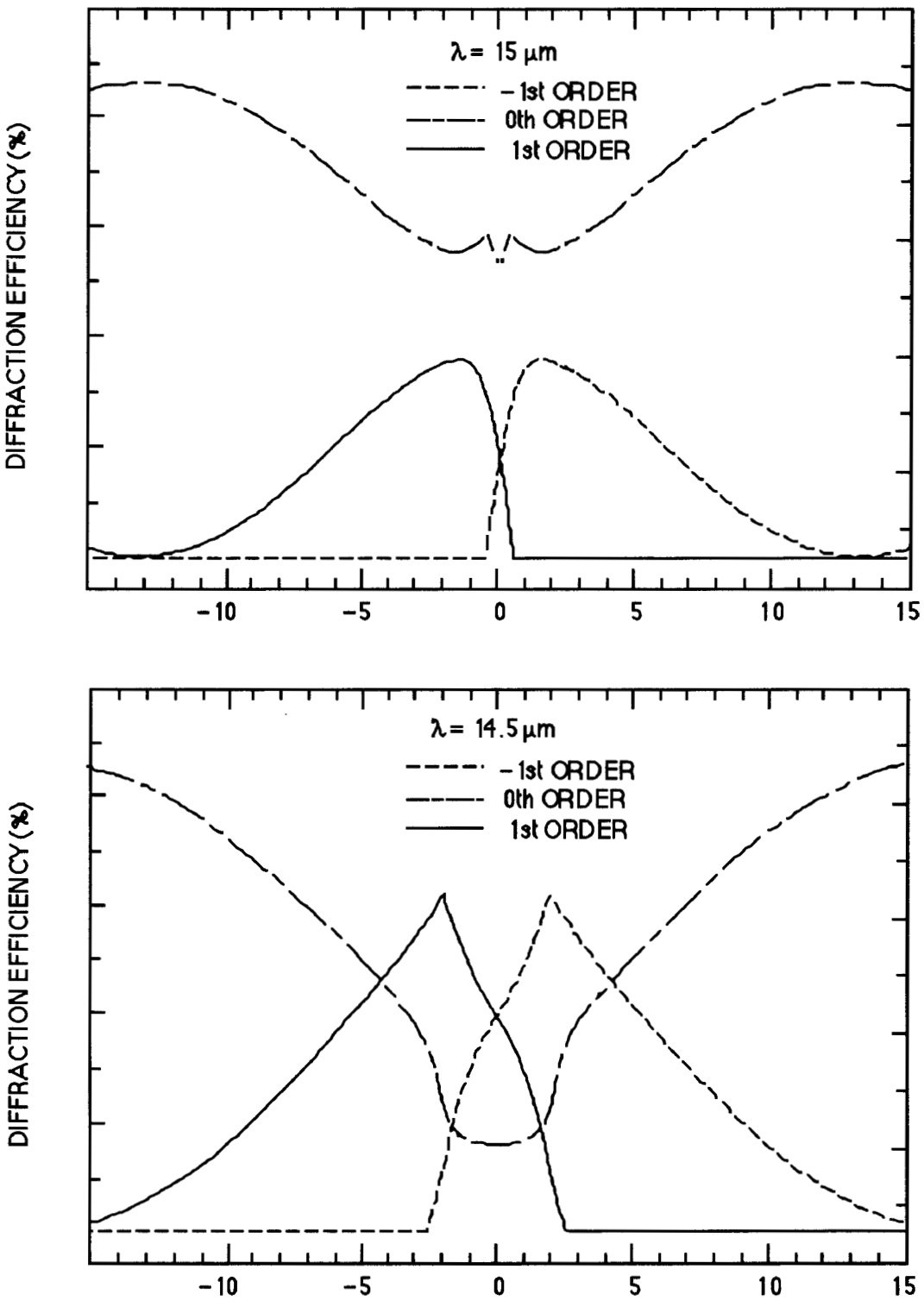


***Fig. 6.*** *Diffraction order efficiencies as a function of incident angle. This data was used together with diffraction angle data to determine the optical coupling (Fig. 1). The grating parameters used in the simulation were period = 4.85 μm, depth = 1.2 μm, and gold fill-factor = 32%.*

## 5. ACKNOWLEDGEMENTS

The research described in this paper was performed by the Center for Space Microelectronics Technology, Jet Propulsion Laboratory, California Institute of Technology, and was jointly sponsored by the Integrated Multispectral Atmospheric Sounder flight project and the National Aeronautics and Space Administration, Office of Space Science.

## 6. REFERENCES

1. B.F. Levine, "Quantum-well Infrared Photodetectors", Journal of Applied Physics vol 74, number 8, p70, 1993.

2. M. B. Stern, M. Holz, S. S. Medeiros, and R. E. Knowlden, "Fabricating binary optcs: process variables critical to optical efficiency," J. Vac. Sci. Technol. B, vol. 9, pp. 3117-3121 (1991).

3. M. B. Stern and S. S. Medeiros, "Deep three-dimensional microstructurefabrication for infrared binary optics," J. Vac. Sci. Technol. B, vol. 10, pp. 2520-2525, 1992.

4. T. Fujita, H. Nishihara, and J. Koyama, "Fabrication of micro lenses using electron-beam lithography," Opt. Lett. 6, 613-615, 1981.

5. M. Ekberg, M. Larsson, S. Hård, and B. Nilsson, "Multilevel phase holograms manufactured by electron beam lithography," Opt. Lett. 15, 568-569, 1990.

6. M. Larsson, M. Ekberg, F. Nikolajeff, and S., Hard, P. D. Maker, and R. E. Muller, "Proximity-compensated kinoforms directly written by E-beam lithography," SPIE Proceedings Vol. CR49, July 1993.

7. P. D. Maker, and R. E. Muller, "Phase holograms in poly methyl methacrylate," J. Vac. Sci. Technol. B 10, 2516-2519, Nov/Dec1992.

8. P. D. Maker and R. E. Muller, "Phase holograms in PMMA with proximity effect correction," NASA CP-3227, 207-221, Feb. 1993.

9. P. D. Maker, D. W. Wilson, and R. E. Muller, "Fabrication and performance of optical interconnect analog phase holograms made be E-beam lithography," in Optoelectronic Interconnects and Packaging, R. T. Chen and P. S. Guilfoyle, eds., SPIE Proceedings vol. CR62, pp. 415-430, Jan. 1996.

10. W. Daschner, M. Larsson, and S. H. Lee, "Fabrication of monolithic diffractive optical elements by the use of E-beam direct write on an analog resist and a single chemically assisted ion-beam etching step," Appl. Opt. 34, 2534-2539, 1995.

11. M.G. Moharam, E.B. Grann, D.A. Pommet, and T.K. Gaylord, "Formulation for stable and efficient implementation of the rigorous coupled-wave analysis of binary gratings," J. Opt. Soc. Am. A, vol. 12, pp. 1068-1076, May 1995.

12. P. Lalanne and G.M. Morris, "Highly improved convergence of the coupled-wave method for TM polarization," J. Opt. Soc. Am. A, vol. 13, pp. 779-784, Apr. 1996.

13. K. Hirayama, E.N. Glytsis, and T.K. Gaylord, "Rigorous electromagnetic analysis of diffraction by finite-number-of-periods gratings," J. Opt. Soc. Am. A, vol. 14, pp. 907-917, Apr. 1997.